Compartmentalization in Atom Transfer Radical Polymerization of Styrene in Dispersed Systems: Effects of Target Molecular Weight and Halide End Group†

Per B. Zetterlund,*,‡ Yasuyuki Kagawa, and Masayoshi Okubo*

Department of Chemical Science and Engineering, Graduate School of Engineering, Kobe University, Kobe 657-8501, Japan

Received January 8, 2009; Revised Manuscript Received February 14, 2009

ABSTRACT: Compartmentalization effects on the kinetics of the atom transfer radical polymerization (ATRP) of styrene employing polystyrene-X/CuX/4,4′-dinonyl-2,2′-dipyridyl (dNbpy) (X = Br or Cl) in a dispersed system at low conversion at 70 or 75 °C have been investigated theoretically using modified Smith−Ewart equations. Compartmentalization always leads to improved livingness (end functionality) because of the segregation effect on propagating radicals reducing the overall termination rate. The control over the molecular weight distribution is, however, only improved if the particles are sufficiently small; that is, a particle size range exists where livingness is improved but control is not. Improved control is obtained as a result of the confined space effect causing an increase in the deactivation rate. The extent of compartmentalization increases with increasing target molecular weight and if Br is replaced with Cl. The present work provides further insight into how one can potentially employ particle size as an experimental parameter to influence ATRP.

Introduction

The implementation of controlled/living radical polymerization (CLRP) in dispersed systems is paramount for the synthesis of nanoparticles comprising polymer of well-defined microstructure as well as for industrial application of CLRP.[1,2] CLRP was originally developed in homogeneous systems (bulk/solution),[3] and CLRP in a dispersed system can proceed quite differently compared with its homogeneous counterpart. There are a number of characteristics of dispersed CLRP systems that are absent in homogeneous systems, for example, compartmentalization and reactant partitioning.[1,2]

Compartmentalization refers to the physical isolation of reactants in discrete confined spaces. Compartmentalization can be subdivided into two separate and distinct effects: the segregation effect and the confined space effect.[4] Segregation refers to two species located in separate particles being unable to react in the absence of a phase transfer event. The confined space effect refers to two species reacting more rapidly in a small particle than in a large particle (a concentration effect). In the emulsion polymerization literature, the term compartmentalization usually refers to segregation of propagating radicals, which is the reason why emulsion polymerizations generally yield higher polymerization rates (R_p) and higher molecular weights (MWs) than bulk/solution polymerizations.[5] The confined space effect is what causes some emulsion polymerizations to be so-called "zero-one" systems.[5,6] As radical entry from the aqueous phase occurs in a particle that already contains a propagating radical, termination takes place before significant propagation occurs, and thus all particles contain either zero or one radical. The confined space effect is also the origin of rapid termination of geminate radicals generated from initiator decomposition in small particles.[7−9]

Compartmentalization in CLRP can be more complex than in nonliving systems depending on whether compartmentalization of the deactivator species also must be considered. The deactivator is compartmentalized if its concentration is sufficiently low and if it is sufficiently insoluble in the continuous phase (usually water).[1] For sufficiently water-soluble deactivators that can diffuse relatively freely between particles, compartmentalization acts on only propagating radicals. This case was theoretically investigated for the nitroxide-mediated polymerization (NMP)[3,10] of styrene at 90 °C by Charleux.[11] For particle diameters of $d < 500$ nm, the termination rate is reduced because of segregation, which results in higher R_p and livingness but a broader molecular weight distribution (MWD). The latter is caused by the reduced deactivation rate (because a lower termination rate leads to less accumulation of free nitroxide) resulting in a higher number of monomer units added per activation−deactivation cycle. These conclusions also apply to atom transfer radical polymerization (ATRP)[3,12,13] when the deactivator (Cu(II) complex) is not compartmentalized.

The case in which both propagating radicals and deactivators are compartmentalized was treated theoretically using modified Smith−Ewart equations for NMP[4,14] and ATRP[15] by Zetterlund and Okubo. In addition to the beneficial effect of segregation of propagating radicals on livingness, the confined space effect may operate on the deactivation reaction, resulting in enhanced deactivation rates. As a consequence, fewer monomer units are added per activation−deactivation cycle, leading to a narrower MWD (for a given molecular weight) and a lower R_p. Butte et al.[16] previously published a similar study on NMP but did not clarify the effects of compartmentalization on the deactivation reaction. The findings by Zetterlund and Okubo were later theoretically verified by Tobita and coworkers using Monte Carlo simulations.[17−19] Moreover, the Monte Carlo technique revealed that fluctuations in the number of deactivators between different particles can lead to a higher overall propagating radical concentration in the organic phase than that predicted from the average deactivator concentration.[17] The findings from the theoretical work described above apply to NMP and ATRP but not reversible addition fragmentation chain transfer (RAFT)[3,20] polymerization. Segregation of propagating radicals influences RAFT polymerization,[21,22] but the confined space effect is normally not operative on deactivation (i.e., the chain transfer step) because of the high concentration of RAFT end groups

† Part 324 of the series "Studies on Suspension and Emulsion".

* Corresponding authors. Tel/Fax: +81-(0)78-803-6161. E-mail: pbztlnd@cx6.scitec.kobe-u.ac.jp (P.B.Z.), okubo@kobe-u.ac.jp (M.O.).

‡ Current address: Centre of Advanced Macromolecular Design, School of Chemical Sciences and Engineering, The University of New South Wales, Sydney, NSW 2052, Australia.

10.1021/ma900035x CCC: $40.75
Published on Web 03/13/2009

(compared with nitroxide in NMP and Cu(II) complex in ATRP).

The general problem when attempting to experimentally detect compartmentalization in ATRP and NMP is that a number of factors may cause deviations compared with the corresponding bulk/solution polymerizations, and it is often difficult to attribute specific effects to compartmentalization. Moreover, the particle size must be sufficiently small, the number of reacting species per particle must be sufficiently low, or both. To date, the strongest experimental evidence of compartmentalization in ATRP was reported by Simms and Cunningham,[23,24] who found that very high MWs (M_n = 989 900, M_w/M_n = 1.25) were obtained in the redox-initiated reverse ATRP of *n*-butyl methacrylate (weight-average diameter <110 nm) in miniemulsion. Current understanding dictates that such high MWs with good control/livingness are not accessible in bulk/solution, and compartmentalization may play a role. Both R_p and M_w/M_n decreased with decreasing particle size, as expected on the basis of the confined space effect.[24] Experimental evidence of compartmentalization effects in NMP has also been reported. Okubo and Zetterlund[25] observed reduced R_p (compared with bulk) in microemulsion NMP of styrene at 125 °C using the nitroxides 2,2,6,6-tetramethylpiperidinyl-1-oxy (TEMPO) and *N-tert*-butyl-*N*-[1-diethylphosphono (2,2-dimethylpropyl)] (SG1). The reduction in R_p was markedly smaller for SG1 than TEMPO, which is consistent with the exit of nitroxide competing more effectively with deactivation for SG1, as expected on the basis of its higher water solubility, and therefore weakening the confined space effect.[26] Cunningham and coworkers[27] reported that as the particle size was decreased in the TEMPO-mediated miniemulsion polymerization of styrene at 135 °C, R_p decreased and the livingness increased, which is consistent with the segregation effect and confined space effect.

We have previously theoretically investigated the ATRP system *n*-butyl acrylate/CuBr/4,4′-dinonyl-2,2′-dipyridyl (dNbpy) at 110 °C for a fixed target MW (briefly described above).[15] The aim of the present contribution is to increase the quantitative understanding of how compartmentalization affects ATRP in dispersed systems by the use of simulations based on modified Smith−Ewart equations, focusing on effects of the target MW and the halide end group (Br or Cl) for the system styrene/(CuBr or CuCl)/dNbpy at 70 or 75 °C. The results are interpreted in terms of the confined space effect and the segregation effect, focusing on how one can exploit compartmentalization to improve control/livingness in ATRP.

Model Development

Bulk/Solution. Bulk/solution ATRP was modeled on the basis of eqs 1−5[12,28]

$$\frac{d[M]}{dt} = -k_p[P^\bullet][M] \quad (1)$$

$$\frac{d[PBr]}{dt} = k_{deact}[P^\bullet][CuBr_2] - k_{act}[PBr][CuBr] \quad (2)$$

$$\frac{d[CuBr]}{dt} = k_{deact}[P^\bullet][CuBr_2] - k_{act}[PBr][CuBr] \quad (3)$$

$$\frac{d[P^\bullet]}{dt} = k_{act}[PBr][CuBr] + k_{i,th}[M]^3 - k_{deact}[P^\bullet][CuBr_2] - 2k_t[P^\bullet]^2 \quad (4)$$

$$\frac{d[CuBr_2]}{dt} = k_{act}[PBr][CuBr] - k_{deact}[P^\bullet][CuBr_2] \quad (5)$$

where M, PBr, and P• are monomer, alkyl halide, and propagating radical, respectively, and k_p, k_{act}, k_{deact}, $k_{i,th}$, and k_t are rate coefficients for propagation, activation, deactivation, thermal (spontaneous) initiation of styrene,[29,30] and termination, respectively. The "2" corresponding to the fact that each thermal initiation event of styrene generates two radicals is included in the value of $k_{i,th}$.

Table 1. Rate Coefficients Employed in the Simulations

	S/CuBr/dNbpy (70 °C)	S/CuBr/dNbpy (75 °C)	S/CuCl/dNbpy (75 °C)
k_{act} (s^{-1})	0.09[a]	0.11[a]	1.66×10^{-3}[b]
k_{deact} ($M^{-1}\cdot s^{-1}$)	1.1×10^{7}[c]	2.5×10^{7}[d]	4.3×10^{6}[e]
k_p($M^{-1}\cdot s^{-1}$)	480[f]	566[f]	566[f]
k_t ($M^{-1}\cdot s^{-1}$)	1.17×10^{8}[g]	1.22×10^{8}[g]	1.22×10^{8}[g]
$k_{i,th}$ ($M^{-2}\cdot s^{-1}$)	6.26×10^{-13}[h]	1.12×10^{-12}[h]	1.12×10^{-12}[h]

[a] Based on E_{act} = 42.1 kJ·mol^{-1} and $A_{act} = 2.2 \times 10^5$ s^{-1} for 1-phenylethylbromide in toluene.[28] [b] Based on k_{act}(1-phenylethylchloride/dNbpy) = 5.6×10^{-5} at 35 °C and k_{act}(1-phenylethylchloride/dHbpy/toluene) = 0.018 at 110 °C (dHbpy = 4,4′-diheptyl-2,2′-bipyridine/acetonitrile), giving E_{act} = 75.5 kJ·mol^{-1} and $A_{act} = 3.56 \times 10^8$ s^{-1}.[28] [c] k_{deact} for polystyryl radical and $CuBr_2$/dHbpy in styrene.[28] [d] k_{deact} for phenylethyl radical and $CuBr_2$/dNbpy in acetonitrile.[28] [e] k_{deact} for phenylethyl radical and $CuCl_2$/dNbpy in acetonitrile.[28] [f] ref 38. [g] ref 39 (based on termination rate = $2k_t[P^\bullet]^2$). [h] ref 29 (based on radical generation rate = $k_{i,th}[S]^3$).

Dispersed System. The model refers to a dispersed system with a constant total number of particles (N_p) of uniform size (i.e., no secondary nucleation, etc.). At time zero, the system comprises N_p monomer droplets, and these are subsequently converted to polymer particles at 1% monomer conversion. As such, strictly speaking, the model corresponds to an ideal miniemulsion polymerization. However, the results can, with caution, also be applied to the polymerization kinetics in polymer particles in other dispersed systems such as emulsion, microemulsion, dispersion, and precipitation polymerizations. The particle formation stage in the above-mentioned dispersed systems is not accounted for in the model, but once particles have formed, the polymerization behavior within these particles with regards to compartmentalization can be understood with the aid of the present simulation results (assuming, of course, that the stoichiometric conditions correspond to those modeled). The system modeled is ideal in the sense that there is no phase transfer between particles (monomer or other reactants). Cu(II) may, in fact, partition significantly between the particles and the continuous phase.[1,31−33] However, to make the task more tractable, we are focusing on compartmentalization effects only.

It was assumed that the number of particles containing ≥4 propagating radicals, ≥31 deactivator species (Cu(II)), or both are negligible. These assumptions hold for all simulations shown; that is, no error is introduced via these assumptions. The model cannot be used for simulations for values of *d* greater than shown in the Figures for the present systems because of the number of deactivator species exceeding the maximum value of 30 in a non-negligible number fraction of particles. The equations were implemented and solved using the software VisSim (version 6.0A11, Visual Solutions) employing numerical integration (backward Euler integration algorithm[34]) with a step size of 1 s and taking great care to ensure minimization of any numerical errors in the simulations. It was ensured that N_p in the simulated system remained constant in all simulations. The values of all rate coefficients employed in the simulations were taken from the literature and are listed in Table 1. The simulations (bulk and dispersed system) were only taken to very low conversion, and as such, conversion-dependences of rate coefficients (mainly k_t[35,36]) need not be included in the model. All rate coefficients were assumed to be independent of chain length. (This assumption would mainly affect k_t (and possibly also k_{deact}), which depends on chain length.[37])

The modified Smith−Ewart equation for ATRP reads[15]

$$\frac{dN_i^j}{dt} = N_A v_p k_{act}[PX][CuX](N_{i-1}^{j-1} - N_i^j) + 0.5k_{i,th}[M]^3 N_A v_p\{N_{i-2}^j - N_i^j\} + \frac{k_t}{N_A v_p}\{(i+2)(i+1)N_{i+2}^j - (i)(i-1)N_i^j\} + \frac{k_{deact}}{N_A v_p}\{(i+1)(j+1)N_{i+1}^{j+1} - (i)(j)N_i^j\} \quad (6)$$

where N_i^j is the number of particles with i P• and j CuX_2, v_p is the particle volume, N_A is Avogadro's number, and X is Br or Cl. The average numbers of P• ($\bar{n}_{P\bullet}$) and CuX_2 ($\bar{n}_{CuX_2}$) per particle are

$$\bar{n}_{P\bullet} = \frac{1}{N_p}\sum_i \sum_j iN_i^j \quad (7)$$

$$\bar{n}_{CuX_2} = \frac{1}{N_p}\sum_i \sum_j jN_i^j \quad (8)$$

where $N_p = \sum_i \sum_j N_i^j$ (the total number of particles). The overall concentrations of P• and CuX_2 in the organic phase are

$$[P\bullet] = \frac{1}{N_A v_p}\frac{1}{N_p}\sum_i \sum_j iN_i^j \quad (9)$$

$$[CuX_2] = \frac{1}{N_A v_p}\frac{1}{N_p}\sum_i \sum_j jN_i^j \quad (10)$$

The propagation step is not affected by compartmentalization (because each particle contains a very high number of monomer units, that is, no confined space effect); therefore, eqs 1 and 9 can be used to compute R_p and monomer conversion. This also applies to the activation reaction between PX and CuX; both reactants are present in high concentration. The concentrations of PX and CuX are thus given by

$$\frac{d[PX]}{dt} = \frac{d[CuX]}{dt} = \frac{k_{deact}}{(N_A v_p)^2}\frac{1}{N_p}\sum_i \sum_j ijN_i^j - k_{act}[PX][CuX] \quad (11)$$

Results and Discussion

Target Molecular Weight Effects on Polymerization Rate. Figure 1 shows simulated conversion time data for the direct ATRP system styrene/PBr/CuBr/dNbpy (70 °C) at different target degrees of polymerization (DP) of 200 ($[PBr]_0$ = 43.5 mM), 2000 ($[PBr]_0$ = 4.35 mM), and 10^4 ($[PBr]_0$ = 0.87 mM). The target DP refers to DP at 100% conversion if the polymerization proceeds in an ideal controlled/living manner as given by $DP_{n,th}$ = ($[monomer]_0/[PBr]_0$) × fractional conversion. Simulated conversion time data for the corresponding bulk systems are also shown. For all target DPs, R_p decreases with decreasing particle size. For very small particles, R_p falls dramatically. If the particle size is increased further than what is shown in Figure 1, then R_p begins to decrease to approach the R_p value in bulk gradually. (See Figure 3 explained later.) For a given particle size (i.e., also in bulk), R_p increases with decreasing target DP (increasing $[PBr]_0$). Moreover, the particle size at which R_p is the same as that in bulk (as seen in Figure 1, i.e., not referring to particles so large that there are no compartmentalization effects) increases with decreasing target DP.

Figure 2 shows the number of propagating radicals and deactivator species per particle. Both quantities dramatically decrease with decreasing particle size to a much greater extent than would be the case if the decreases were merely caused by the reduction in particle volume itself in the absence of any kinetic effects. The values of $\bar{n}_{P\bullet}$ remain below 0.003 under all conditions investigated, whereas $\bar{n}_{CuBr_2}$ reaches values as high as 5. The vast majority of particles contain no propagating radical at a given time.

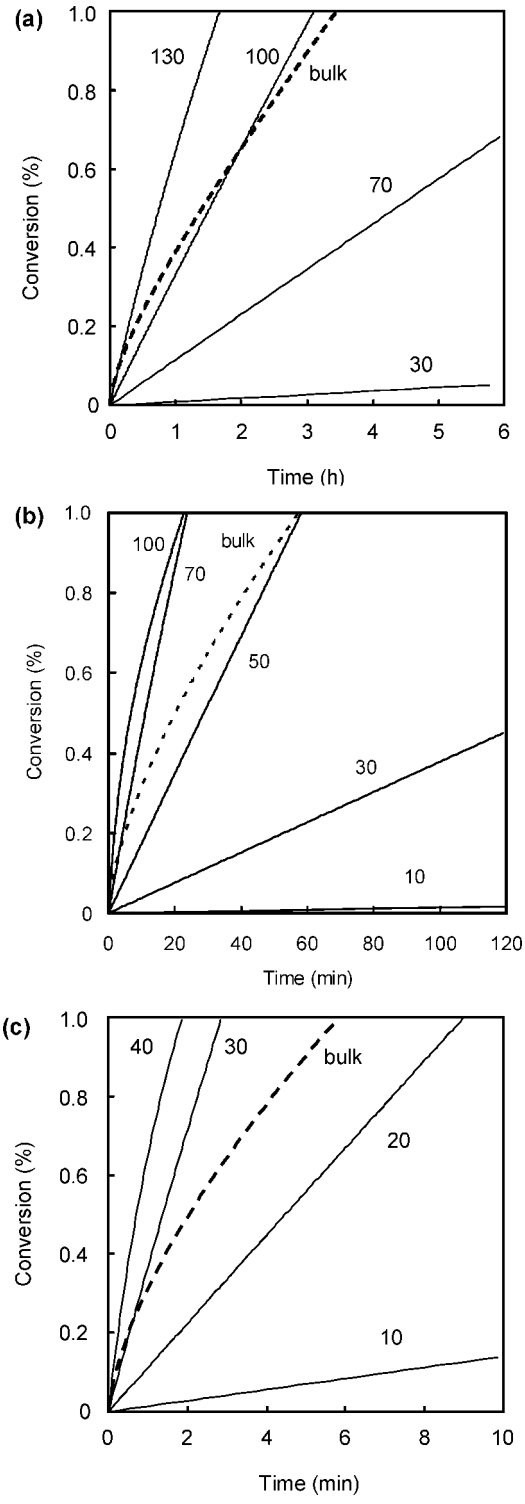

Figure 1. Simulated conversion versus time data for ATRP of styrene ($[styrene]_0$ = 8.7 M in organic phase) at 70 °C in a dispersed system as a function of particle diameter (indicated in nanometers) and in bulk (dotted line): (a) $[PBr]_0 = [CuBr/dNbpy]_0$ = 0.87 mM, (b) $[PBr]_0 = [CuBr/2dNbpy]_0$ = 4.35 mM, and (c) $[PBr]_0 = [CuBr/2dNbpy]_0$ = 43.5 mM. Theoretical degrees of polymerization at 100% conversion: (a) 10^4; (b) 2000, and (c) 200. The *y* axes are in percentage conversion, not fractional conversion (i.e., max conversion shown is 1%).

Criteria for Confined Space Effect on Deactivation. An alternative way of examining the conversion time data is to

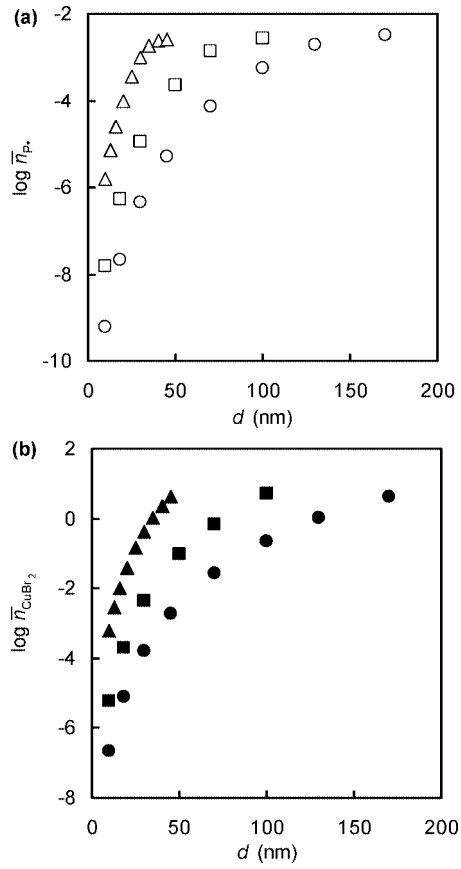

Figure 2. Simulated average numbers of (a) P• and (b) $CuBr_2$ per particle at 1% conversion as a function of particle diameter (d) for ATRP of styrene ([styrene]$_0$ = 8.7 M in organic phase) in a dispersed system at 70 °C with [PBr]$_0$ = [CuBr/2dNbpy]$_0$ = 0.87 (○, ●), 4.35 (■, □), and 43.5 (△, ▲) mM.

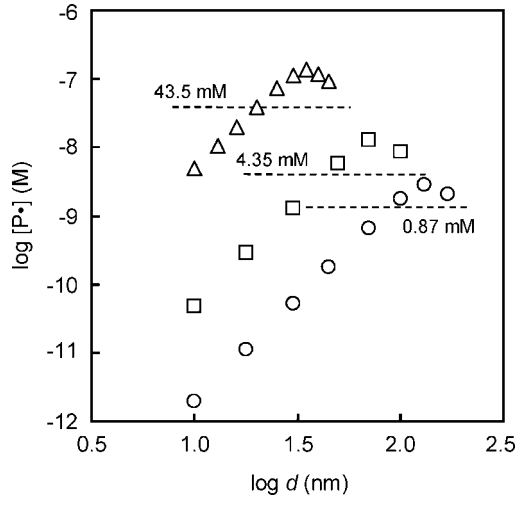

Figure 3. Simulated [P•] as a function of particle diameter at 1% conversion for ATRP of styrene ([styrene]$_0$ = 8.7 M in organic phase) in a dispersed system at 70 °C at [PBr]$_0$ = [CuBr/2dNbpy]$_0$ = 0.87 (○), 4.35 (□), and 43.5 (△) mM. The broken lines indicate [P•] at 1% conversion in bulk.

instead plot log[P•] versus log d (Figure 3). ([P•] is proportional to R_p in both bulk and dispersed systems.) In the dispersed system, [P•] refers to the overall concentration of propagating radicals in the organic phase. As described and explained previously for the ATRP system *n*-butyl acrylate/CuBr/dNbpy/(110 °C)[15] and the NMP system styrene/TEMPO (125 °C),[4,14] log[P•] increases linearly with log d for small particles with a slope equal to 3, goes through a maximum, and then gradually approaches the bulk value as d further increases. The particle size where compartmentalization becomes important decreases with decreasing DP (increasing [PBr]$_0$). Therefore, when DP = 10^4 is targeted, compartmentalization exerts significant influence when $d < \sim$220 nm. However, for DP = 200, particles as small as d < 55 nm are required for compartmentalization to play a role. These "critical" particle sizes correspond to $\bar{n}_{P\bullet} \approx 0.003$ and $\bar{n}_{CuBr_2} \approx 5$ (Figures 2 and 3). In other words, regardless of the targeted DP (i.e., [PBr]$_0$, the concentration of living chains), compartmentalization effects set in when the values of $\bar{n}_{P\bullet}$ and $\bar{n}_{CuBr_2}$ decrease below certain values.

With regards to the confined space effect on deactivation, the "critical" value of $\bar{n}_{CuBr_2}$ is independent of the particular system. The overall deactivation rate increases as a result of the confined space effect (relative to the corresponding bulk system) when some particles do not contain any $CuBr_2$; that is, the volume of the particles without $CuBr_2$ is "excluded" from the system, thus giving a higher [$CuBr_2$] in the particles that do contain $CuBr_2$. This is expressed in eq 12[17]

$$v_{p,crit} < \frac{1}{N_A[CuBr_2]_{bulk}} \tag{12}$$

where $v_{p,crit}$ denotes the maximum v_p where the confined space effect on deactivation operates at a given [$CuBr_2$]$_{bulk}$. The value of $v_{p,crit}$ corresponds to when $\bar{n}_{CuBr_2} = 1$ (= [$CuBr_2$]$N_A v_{p,crit}$). In a system based on averages $\bar{n}_{CuBr_2}$= 1 means that all particles contain one $CuBr_2$. In a real system, however, there will be variations in the number of $CuBr_2$ between particles, and even if $\bar{n}_{CuBr_2}$= 1, some particles would contain zero $CuBr_2$, whereas others would contain two or three or more. As a consequence, in a real system, the confined space effect may operate at $v_p > v_{p,crit}$, and this is important to keep in mind when comparing theory and experiment. The present rationale also applies to NMP as well as to all CLRP based on the persistent radical effect (i.e., not RAFT).

Compartmentalization Effects on Deactivation and Termination. Figure 4 displays the rates of deactivation and termination relative to the corresponding rates in a homogeneous system calculated on the basis of eqs 13−16[4,15]

$$R_{deact}^{c} = \frac{k_{deact}}{(N_A v_p)^2}\frac{1}{N_p}\sum_i \sum_j ijN_i^j \tag{13}$$

$$R_t^{c} = \frac{2k_t}{(N_A v_p)^2}\frac{1}{N_p}\sum_i \sum_j i(i-1)N_i^j \tag{14}$$

$$R_{deact}^{nc} = k_{deact}[P\bullet][CuBr_2] \tag{15}$$

$$R_t^{nc} = 2k_t[P\bullet]^2 \tag{16}$$

R^c denotes the compartmentalized rate, whereas R^{nc} is the rate if all compartmentalization effects are "removed" instantaneously. (All particles are instantaneously combined into a continuous organic phase.) For sufficiently large particles, $\log(R^c/R^{nc}) = 0$ ($R^c = R^{nc}$) for both deactivation and termination; that is, there are no effects of compartmentalization. For sufficiently small particles, the deactivation rate increases relative to the corresponding homogeneous system because of the confined space effect. As the particle size is reduced, segregation leads to a reduction in the relative termination rate, and upon further reduction in particle size, the value of $\log(R^c/R^{nc})$ goes through a minimum, and eventually $\log(R^c/R^{nc}) > 0$ for very small particles (Figure 4a). Thermal (spontaneous) initiation of styrene proceeds at a low rate at 70 °C[29] but cannot

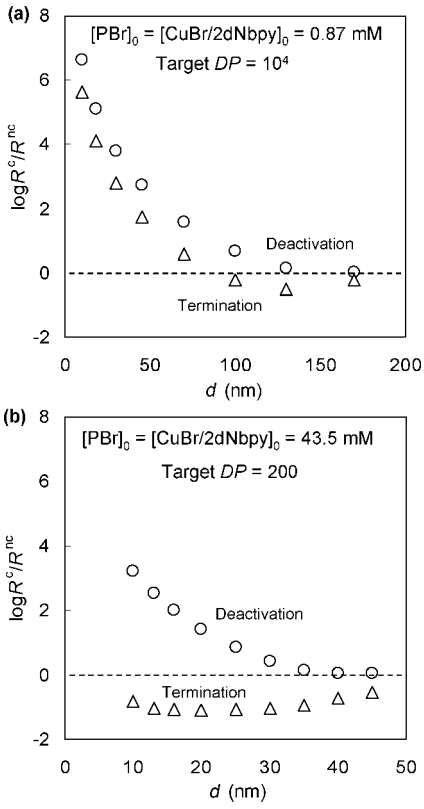

Figure 4. Ratios of simulated "compartmentalized" and "noncompartmentalized" deactivation (○) and termination (△) rates as functions of particle diameter (d) at 1% conversion for ATRP of styrene ([styrene]$_0$ = 8.7 M in organic phase) at 70 °C with [PBr]$_0$ = [CuBr/2dNbpy]$_0$ = (a) 0.87 and (b) 43.5 mM. R superscripts: c is compartmentalized; nc is noncompartmentalized. The dotted lines indicate $R^c = R^{nc}$.

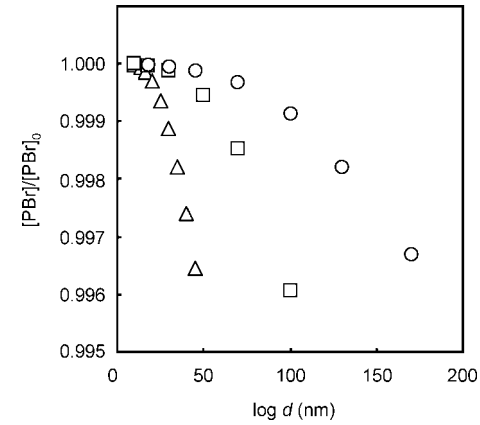

Figure 5. Simulated fraction of "living" polymer chains as a function of particle diameter at 1% conversion for ATRP of styrene ([styrene]$_0$ = 8.7 M in organic phase) in a dispersed system at 70 °C with [PBr]$_0$ = [CuBr/2dNbpy]$_0$ = 0.87 (○), 4.35 (□), and 43.5 (△) mM.

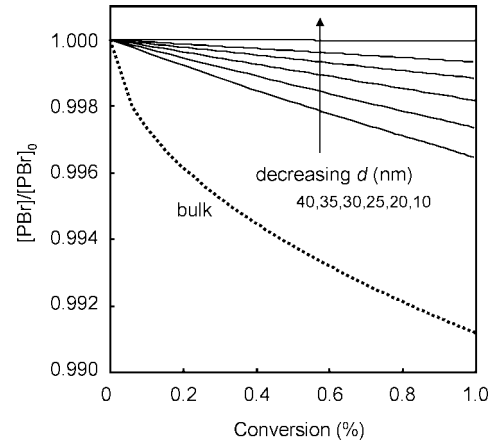

Figure 6. Simulated fraction of "living" polymer chains as a function of conversion for ATRP of styrene ([styrene]$_0$ = 8.7 M in organic phase) in a dispersed system at 70 °C with [PBr]$_0$ = [CuBr/2dNbpy]$_0$ = 43.5 mM. The dotted line denotes bulk conditions. The x axis is in percentage conversion, not fractional conversion (i.e., max conversion shown is 1%).

be neglected. These thermal radicals are generated in pairs, and the rate of geminate termination increases with decreasing particle size; this is also the confined space effect. In the model, the overall termination rate is the sum of all radical−radical coupling reactions (except deactivation), and for sufficiently small particles, the increase in geminate termination rate of thermal radicals outweighs the reduction in termination by segregation of radicals generated from activation of alkyl halide species. This is why $\log(R^c/R^{nc})$ for termination passes through a minimum as the particle size is reduced (Figure 4) and in some cases leads to $R^c > R^{nc}$ (Figure 4a).

At [PX]$_0$ of both 43.5 and 0.87 mM, the segregation effect begins to exert an influence at greater particle sizes than the confined space effect. A maximum in [P•] and R_p occurs in the particle size region where the segregation effect on termination is stronger than the confined space effect on deactivation (Figures 1 and 3). The size of the maximum in [P•] relative to the bulk value increases with increasing [PX]$_0$ (decreasing DP) (Figure 3). The relative contribution of spontaneously generated radicals to the overall termination rate is greater at the lower [PX]$_0$, which explains why $\log(R^c/R^{nc})$ for termination is lower for [PX]$_0$ = 43.5 mM (Figure 4b) than for [PX]$_0$ = 0.87 mM (Figure 4a). Consequently, the maximum in [P•] (relative to bulk) increases with increasing [PX]$_0$ in Figure 3.

Tobita has argued that for the NMP system styrene/TEMPO (125 °C), the maximum in R_p is mainly caused by the fluctuation effect.[17] Fluctuation in the number of deactivator species (Cu(II) in the case of ATRP, nitroxide in NMP) between particles can result in a higher overall [P•] (and R_p) than predicted from the average number of deactivators per particle. Such fluctuations are accounted for by the Smith−Ewart equations approach. (It has previously been incorrectly stated that the Smith−Ewart equations do not account for fluctuation effects.[1]) Fluctuation in the number of deactivators between particles influences the way in which the overall deactivation and termination rates are affected by compartmentalization. However, the fundamental reasons why R_p and [P•] are different in a compartmentalized system than in bulk are the confined space effect and the segregation effect, and the maxima in R_p and [P•] can be fully explained on the basis of the compartmentalization effects on deactivation and termination as in Figures 4 and 11.

Degree of Livingness. Figure 5 shows the fraction of alkyl halide species relative to the initial amount, that is, the livingness, at a fixed conversion of 1% as a function of particle diameter for various [PX]$_0$. The livingness is considerably higher than one would observe by experiment because (1) the conversion is very low and (2) various side reactions lead to loss of livingness, and these are not included in the model.[3] For a given [PX]$_0$, the livingness increases with decreasing particle size as a result of segregation of propagating radicals reducing the termination rate. At a given particle size, the livingness increases with decreasing [PX]$_0$. Figure 6 shows how the livingness decreases with increasing conversion for [PX]$_0$ = 43.5 mM and how this decrease is much less severe for smaller particles. These results are best understood by inspection of the data in Figure 4 (or Figure 3). For a lower [PX]$_0$, the segregation effect becomes important at a greater particle size than that for a higher

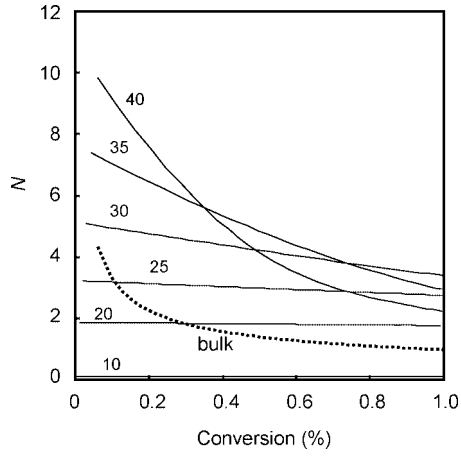

Figure 7. Simulated number of propagation events per activation−deactivation cycle (N) for an individual chain as a function of conversion for ATRP of styrene ([styrene]$_0$ = 8.7 M in organic phase) in a dispersed system at 70 °C with [PBr]$_0$ = [CuBr/2dNbpy]$_0$ = 43.5 mM for different particle diameters (indicated in nanometers). The dotted line denotes bulk conditions. Note that the x axis is in percentage conversion, not fractional conversion (i.e., max conversion shown is 1%).

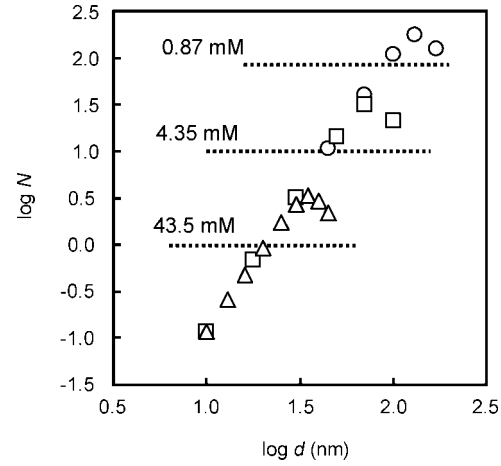

Figure 8. Simulated number of propagation events per activation−deactivation cycle for an individual chain (N) as a function of particle diameter (d) at 1% conversion for ATRP of styrene ([styrene]$_0$ = 8.7 M in organic phase) in a dispersed system at 70 °C with [PBr]$_0$ = [CuBr/2dNbpy]$_0$ = 0.87 (○), 4.35 (□), and 43.5 (△) mM. The dotted lines show N at 1% conversion in bulk.

[PX]$_0$. It follows that for a given particle size, the segregation effect is stronger for the system with a lower [PX]$_0$, which thus has higher livingness.

Degree of Control. The MWDs are not computed by the present model. However, the degree of control can be assessed via examination of the number of propagation events per activation−deactivation cycle for an individual chain (N)[4]

$$N = \frac{k_p[M][P^\bullet]}{(N_A v_p)^{-2} k_{deact} \sum_i \sum_j ijN_i^j} = \frac{k_p[M](N_A v_p)^{-1} \sum_i iN_i}{(N_A v_p)^{-2} k_{deact} \sum_i \sum_j ijN_i^j} = \frac{k_p[M] \sum_i iN_i}{(N_A v_p)^{-1} k_{deact} \sum_i \sum_j ijN_i^j} \quad (17)$$

where $(N_A v_p)^{-1} \sum iN_i = [P^\bullet]$. In ideal CLRP, that is, in the absence of termination, transfer, and other side reactions, M_w/M_n decreases with an increasing number of activation−deactivation cycles as polymer chains grow.[28] Therefore, for a given molecular weight, M_w/M_n decreases with decreasing N. Figure 7 shows N versus conversion for [PX]$_0$ = 43.5 mM, revealing how N generally decreases with decreasing particle size because of the confined space effect causing an increase in the deactivation rate. For very small particles (d < 20 nm), N is lower than that in bulk. The reason N is higher than that in bulk for d > 20 nm is that segregation results in a reduced termination rate, which in turn causes the accumulation of deactivator species (Cu(II)) to decrease, and thus the deactivation rate decreases. For very small particles, the confined space effect on deactivation is strong enough to overcome this indirect effect of segregation on the deactivator concentration, and thus N is lower than that in bulk. N decreases with increasing conversion because of the deactivator concentration increasing with time (because of termination). The decrease in N with conversion is weaker for small particles because the segregation effect on termination limits the build up in the deactivator concentration.

The values of N are plotted versus particle diameter in a log−log plot for the three different [PX]$_0$ in Figure 8. For sufficiently small particles, $N_0^0 + N_1^1 = N_{tot}$, and the termination rate is negligible. It has previously been shown theoretically[4] for the analogous case in NMP that under such conditions, a plot of log[P•] versus log d (Figure 3) gives a straight line with a slope of 3. In the case of [PX]$_0$ = 0.87 mM, this is the case for d < ~100 nm. Now, if one examines a single particle containing one propagating radical and one deactivator molecule for a given activation rate, then R_p in that particle is proportional to N. The value of N is, in turn, inversely proportional to the deactivation rate, which is given by $k_{deact}/N_A v_p$, which is proportional to $1/d^3$. Consequently, a plot of log N versus log d yields a straight line with a slope of 3 (from the term $1/d^3$) for sufficiently small particles. When $N_0^0 + N_1^1 = N_{tot}$ and the termination rate is negligible, N is independent of [PBr]$_0$, as evidenced by the linear portions of all plots falling on the same master curve. Under such conditions, no second activation event occurs during the time between activation and deactivation of a given PBr species, and it follows that the number of propagation steps that occur prior to deactivation is independent of the number of dormant PBr species. As [PBr]$_0$, the particle size, or both increase, it becomes more likely that a second activation event occurs during an active period, and the conditions of $N_0^0 + N_1^1 = N_{tot}$ and negligible termination rate thus no longer hold. This is why the straight lines begin to deviate downward in Figure 8 when d is too high. The higher the value of [PBr]$_0$, the lower the particle size where this occurs.

The plot of log[P•] versus log d (Figure 3) looks very similar to the plot of log N versus log d (Figure 8), with the slope also being equal to 3 for sufficiently small particles. However, in the case of log[P•] versus log d, the straight portions of the plots do not form a master curve. At a given particle size, an increase in [PT]$_0$ leads to an increase in [P•], although N remains unchanged. Now, the value of [P•] refers to the overall concentration in the organic phase, and an increase in [PT]$_0$ therefore leads to an increase in N_1^1, and thus no master curve is formed even if $N_0^0 + N_1^1 = N_{tot}$ and the termination rate is negligible.

Effects of Halide End Group (Br versus Cl). Simulations were carried out as above for both PBr and PCl at 75 °C (rate coefficients for PCl not available at 70 °C) to elucidate how the halide end group affects the influence of compartmentalization on ATRP. The type of halide end group affects ATRP in that it greatly influences the activation−deactivation process. According to the literature, the values of k_{act} and k_{deact} are 66 and 5.8 times higher, respectively, for Br than for Cl (Table 1).

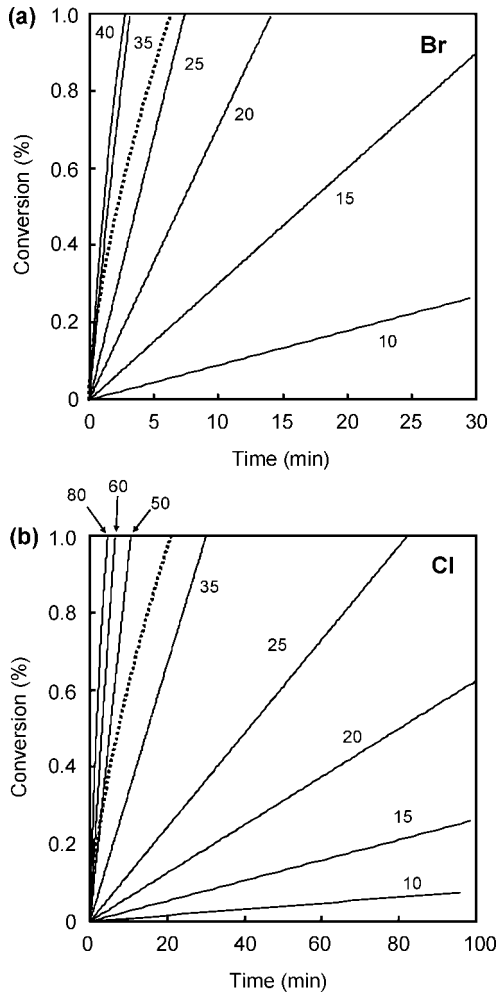

Figure 9. Simulated conversion versus time data for ATRP of styrene ([styrene]$_0$ = 8.7 M in organic phase) at 75 °C in a dispersed system as a function of particle diameter (indicated in nanometers) and in bulk (dotted lines): (a) [PX]$_0$ = [CuBr/2dNbpy]$_0$ = 43.5 mM and (b) [PX]$_0$ = [CuCl/2dNbpy]$_0$ = 43.5 mM. Note that the *y* axis is in percentage conversion, not fractional conversion (i.e., max conversion shown is 1%).

As expected, R_p was considerably higher for Br than for Cl both in the bulk and dispersed systems (Figure 9). The effect of particle size on R_p is principally the same as that explained in connection with Figure 1. It is easier to compare the two systems by examining the plots of log[P•] versus log *d* (Figure 10): (1) The plots show the same trends, but the plot for Cl is shifted to greater *d* values compared with the plot for Br. (2) The maximum value (relative to bulk) is greater for Cl than for Br. The results can be understood by again examining the rates of deactivation and termination relative to the corresponding bulk systems (Figure 11).

In the case of Cl, the confined space effect and the segregation effect begin to influence deactivation and termination, respectively, at greater *d* than for Br. On the basis of the literature values employed (Table 1), k_{act}/k_{deact} is 11.4 times greater for Br. An increase in k_{act}/k_{deact} results in an increase in both $\bar{n}_{P\cdot}$ and $\bar{n}_{CuBr_2}$, and it follows that smaller particle sizes are required for Br than for Cl for compartmentalization (both confined space effect and segregation) to become significant. These results are analogous to previously reported theoretical findings on the effect of increasing the macroinitiator concentration in NMP in dispersed systems.[14]

The segregation effect on termination is stronger for Cl than for Br (i.e., $\log(R^c/R^{nc})$ for termination is lower for Cl than for

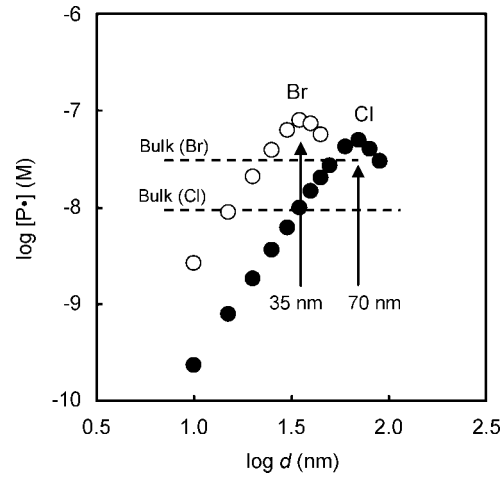

Figure 10. Simulated [P•] as a function of particle diameter (*d*) at 1% conversion for ATRP of styrene ([styrene]$_0$ = 8.7 M in organic phase) at 75 °C in a dispersed system as a function of particle diameter (*d*) and in bulk (dotted lines): [PX]$_0$ = [CuBr/2dNbpy]$_0$ = 43.5 mM (○) and [PX]$_0$ = [CuCl/2dNbpy]$_0$ = 43.5 mM (●). The dotted lines indicate [P•] in bulk of the respective bulk systems at 1% conversion.

Br at the minimum value in Figure 11), which explains why the maximum in R_p is greater for Cl than for Br. The extent of the segregation effect, as estimated by $\log R^c/R^{nc}$, is a complex function of $\bar{n}_{P\cdot}$ in the dispersed system and [P•] in the corresponding bulk system. Consider that a bulk system is instantaneously converted to a dispersed system by dividing the system into discrete units (particles). If [P•] is too high, then there will be no segregation effect in the dispersed system because $\bar{n}_{P\cdot}$ is too high; that is, the propagating radicals are not sufficiently segregated. However, at the other extreme at infinite dilution, the effect of segregation will be small because the propagating radicals are already very "segregated" in the bulk system (and the termination rate is proportional to [P•]^2). Therefore, one can expect that a plot of $\log(R^c/R^{nc})$ versus [P•] (or the corresponding $\bar{n}_{P\cdot}$) would go through a maximum, and an increase in [P•] may thus lead to an increase or decrease in $\log(R^c/R^{nc})$ depending on the particular conditions. In the present systems, the values of $\bar{n}_{P\cdot}$ at the point where the segregation effects are the strongest (Figure 11) are: $\bar{n}_{P\cdot} = 1.9 \times 10^{-4}$ (Br, d = 25 nm) and 1.07×10^{-3} (Cl, d = 50 nm). As mentioned earlier, an additional factor is the contribution of geminate termination of radicals generated in pairs by spontaneous initiation of styrene. These radicals rapidly terminate in small particles because of the confined space effect, and this termination is included in the overall termination rate,[4] which is why $\log(R^c/R^{nc})$ eventually increases as *d* decreases (beyond the minimum in $\log(R^c/R^{nc})$) in Figure 11.

The effect of Cl versus Br on the livingness at a fixed conversion as a function of *d* is displayed in Figure 12. The livingness is higher for Cl than for Br; that is, the extent of bimolecular termination is greater for Br than Cl. The livingness can be correlated with $\bar{n}_{P\cdot}$; the lower the value of $\bar{n}_{P\cdot}$, the higher the livingness because the stronger the segregation effect on termination. It can be seen in Figure 13 that at a given *d*, $\bar{n}_{P\cdot}$ is higher for Br than for Cl. However, there will be a particle size region of approximately $50 < d < \sim 80$ nm where $\bar{n}_{P\cdot}(Cl) > \bar{n}_{P\cdot}(Br)$, as can be predicted from Figure 10. This is the particle size region in Figure 10 corresponding to the maximum in log[P•] for Cl and the approach to bulk conditions for Br as *d* is increased.

The control, again assessed via the parameter *N*, is examined in Figure 14. Both in bulk and for a given particle size, *N* is much greater for Cl than for Br. In bulk, [P•] is much lower for Cl than for Br (Figure 10), and it follows that less termination

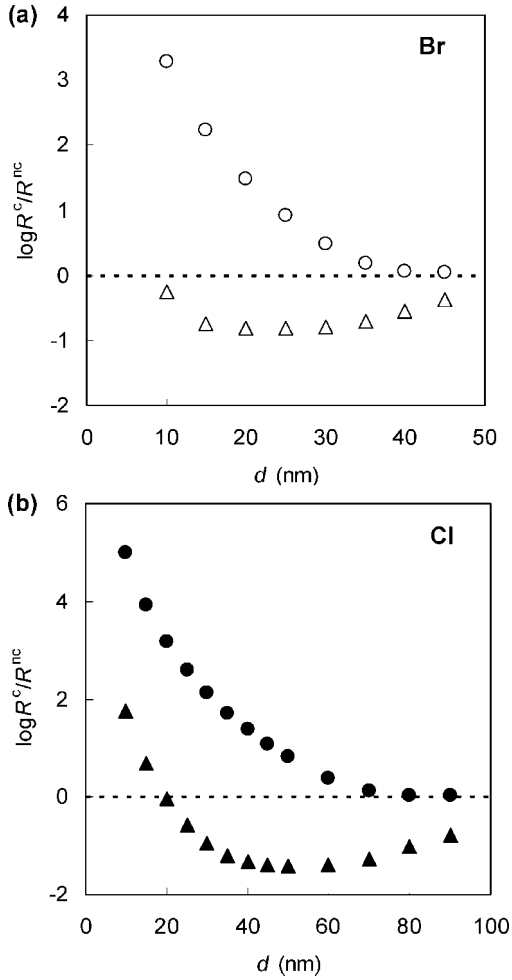

Figure 11. Ratios of simulated "compartmentalized" and "noncompartmentalized" deactivation (○, ●) and termination (△, ▲) rates as a function of particle diameter (d) at 1% conversion for ATRP of styrene ($[\text{styrene}]_0 = 8.7$ M in organic phase) at 75 °C with (a) $[\text{PX}]_0 = [\text{CuBr/2dNbpy}]_0 = 43.5$ mM and (b) $[\text{PX}]_0 = [\text{CuCl/2dNbpy}]_0 = 43.5$ mM. R superscripts: c is compartmentalized; nc is noncompartmentalized. The dotted lines indicate $R^c = R^{nc}$.

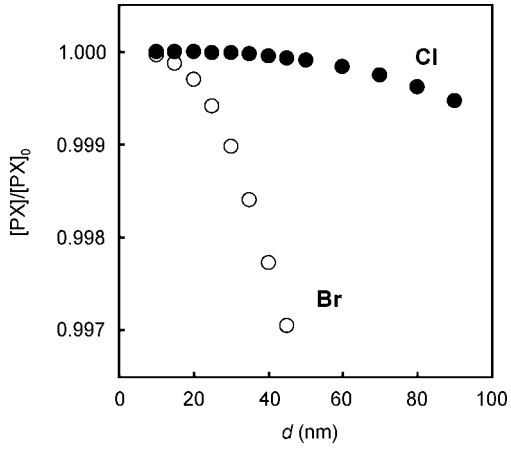

Figure 12. Simulated fraction of "living" polymer chains as a function of particle diameter (d) at 1% conversion for ATRP of styrene ($[\text{styrene}]_0 = 8.7$ M in organic phase) at 75 °C with $[\text{PX}]_0 = [\text{CuBr/2dNbpy}]_0 = 43.5$ mM (○) and $[\text{PX}]_0 = [\text{CuCl/2dNbpy}]_0 = 43.5$ mM (●).

occurs for Cl than for Br. This in turn means that the concentration of Cu(II) is lower for Cl than for Br. (An increase in termination rate leads to an increase in deactivator concentration as dictated by the persistent radical effect.[28]) Moreover, $k_{deact}(\text{Cl}) < k_{deact}(\text{Br})$ on the basis of the literature values employed. The deactivation rate is therefore lower for Cl than

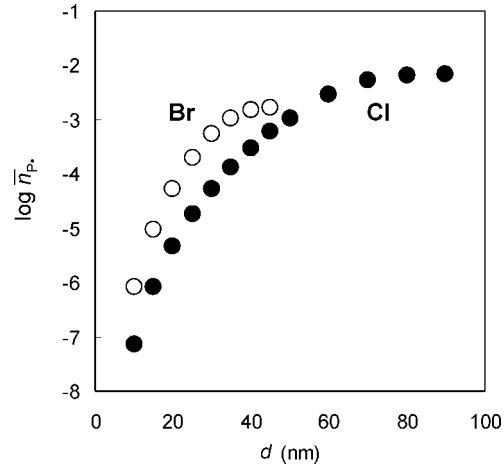

Figure 13. Simulated average numbers of P• per particle at 1% conversion as a function of particle diameter (d) for ATRP of styrene ($[\text{styrene}]_0 = 8.7$ M in organic phase) at 75 °C with $[\text{PX}]_0 = [\text{CuBr/2dNbpy}]_0 = 43.5$ mM (○) and $[\text{PX}]_0 = [\text{CuCl/2dNbpy}]_0 = 43.5$ mM (●).

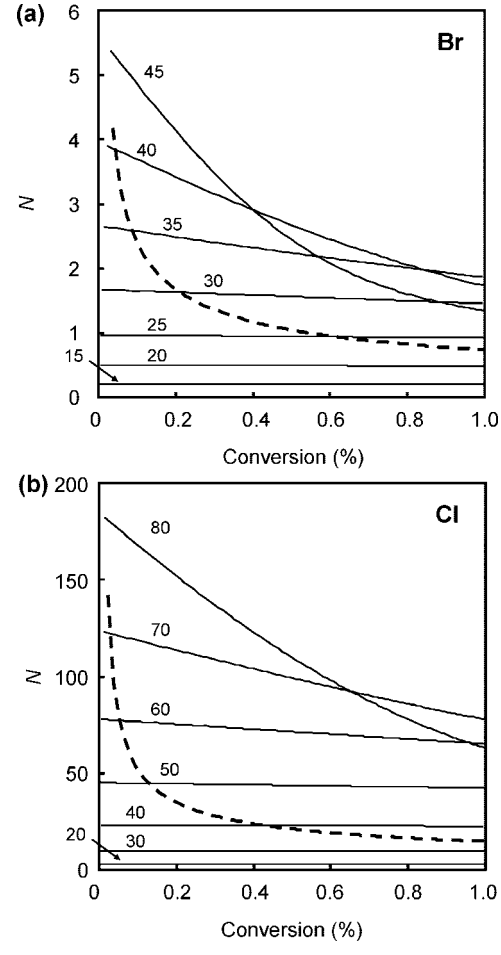

Figure 14. Simulated number of propagation events per activation-deactivation cycle (N) for an individual chain as a function of conversion for ATRP of styrene ($[\text{styrene}]_0 = 8.7$ M in organic phase) in a dispersed system at various particle diameters (indicated in nanometers) at 75 °C with (a) $[\text{PX}]_0 = [\text{CuBr/2dNbpy}]_0 = 43.5$ mM and (b) $[\text{PX}]_0 = [\text{CuCl/2dNbpy}]_0 = 43.5$ mM. The dotted lines denote bulk conditions. Note that the x axis is in percentage conversion, not fractional conversion (i.e., max conversion shown is 1%).

for Br for the above two reasons, and thus the value of N is higher than that for Br. For a given particle size, N is higher for Cl than for Br for the same reasons as in bulk. Therefore, it is predicted that in the idealized cases modeled, the level of control would be better for Br (Figure 14), but the livingness would be better for Cl (Figure 12). For Br, $d < \sim 25$ nm is required for N to be lower than that in bulk (because of the confined space effect on deactivation), whereas for Cl, $d < \sim 30$ nm. The increase in deactivation rate due to the confined space effect is thus stronger for Cl than for Br. This can be readily understood in terms of eq 13; the organic phase concentration of Cu(II) is lower for Cl than for Br; therefore, the confined space effect is stronger for Cl. This can also be inferred from Figure 11: for a given particle size, the value of $\log(R^c/R^{nc})$ for deactivation is greater for Cl than for Br (except for particles so large that $\log(R^c/R^{nc}) = 1$ for Cl).

Conclusions

Extensive modeling and simulations have been performed using modified Smith−Ewart equations to investigate the effects of compartmentalization (the confined space effect and the segregation effect) on the kinetics of the ATRP of styrene at low conversion employing polystyrene-X/CuX/4,4′-dinonyl-2,2′-dipyridyl (dNbpy) (X = Br or Cl) in a dispersed system at 70 or 75 °C.

Under conditions at which compartmentalization exerts an effect on the kinetics, the livingness is always improved as a result of the reduced bimolecular termination rate caused by segregation of propagating radicals. The level of control over the MWD (the narrowness) may be better or worse than the corresponding bulk system. If the particles are sufficiently small, then the control is better. However, for larger particles (yet so small that the segregation effect is operative), broader MWDs result. Under conditions at which the control is improved, the polymerization rate is lower than that in bulk and vice versa. The confined space effect acts as to reduce the polymerization rate by increasing the deactivation rate, whereas the opposite is true for the segregation effect on termination. For the system with $[PBr]_0 = 43.5$ mM at 70 °C, the livingness is improved relative to bulk for $d < \sim 55$ nm, whereas the control is improved when $d < \sim 20$ nm.

The maximum particle size (d_{max}) at which compartmentalization exerts an influence on the kinetics increases with increasing target degree of polymerization (DP), that is, with decreasing $[PBr]_0$ (concentration of living chains). For $[PBr]_0 = 43.5$ M (DP = 200 at 100% conversion), $d_{max} = 55$ nm, and for $[PBr]_0 = 0.87$ mM (DP = 10^4 at 100% conversion), $d_{max} = 220$ nm. Moreover, the onset of compartmentalization effects occurs for larger particles for Cl than for Br as the alkyl end group. With $[PX]_0 = 43.5$ mM (X = Br or Cl), $d_{max} > 100$ nm for Cl and 55 nm for Br. Both of these effects have the same origin; for compartmentalization to be significant, the number of propagating radicals (segregation effect) and deactivator species (confined space effect) per particle must be sufficiently low. An increase in $[PX]_0$ results in an increase in both quantities. The ATRP equilibrium for the Br system lies more to the active state than the Cl system, and thus the concentrations of propagating radicals and deactivator species are higher for Br than Cl.

The results presented further deepen the theoretical understanding of compartmentalization effects in dispersed ATRP systems and offer means of how it may be possible to improve both control and livingness by employing particle size as an experimental parameter.

Acknowledgment. This work was partially supported by a Grant-in-Aid for Scientific Research (19550125) from the Japan Society for the Promotion of Science (JSPS), a Research Fellowship of the JSPS for Young Scientists (Y.K.), and a Kobe University Takuetsu-shita Research Project.

References and Notes

(1) Zetterlund, P. B.; Kagawa, Y.; Okubo, M. *Chem. Rev.* **2008**, *108*, 3747–3794.
(2) Cunningham, M. F. *Prog. Polym. Sci.* **2008**, *33*, 365–398.
(3) Braunecker, W. A.; Matyjaszewski, K. *Prog. Polym. Sci.* **2007**, *32*, 93–146.
(4) Zetterlund, P. B.; Okubo, M. *Macromolecules* **2006**, *39*, 8959–8967.
(5) Gilbert, R. G. *Emulsion Polymerization: A Mechanistic Approach*; Academic Press: London, 1995.
(6) Maeder, S.; Gilbert, R. G. *Macromolecules* **1998**, *31*, 4410–4418.
(7) Luo, Y.; Schork, F. J. *J. Polym. Sci., Part A: Polym. Chem.* **2002**, *40*, 3200–3211.
(8) Nomura, M.; Suzuki, K. *Ind. Eng. Chem. Res.* **2005**, *44*, 2561–2567.
(9) Autran, C.; de-la-Cal, J. C.; Asua, J. M. *Macromolecules* **2007**, *40*, 6233–6238.
(10) Georges, M. K.; Veregin, R. P. N.; Kazmaier, P. M.; Hamer, G. K. *Macromolecules* **1993**, *26*, 2987–2988.
(11) Charleux, B. *Macromolecules* **2000**, *33*, 5358–5365.
(12) Matyjaszewski, K.; Xia, J. *Chem. Rev.* **2001**, *101*, 2921–2990.
(13) Kamigaito, M.; Ando, T.; Sawamoto, M. *Chem. Rev.* **2001**, *101*, 3689.
(14) Zetterlund, P. B.; Okubo, M. *Macromol. Theory Simul.* **2007**, *16*, 221–226.
(15) Kagawa, Y.; Zetterlund, P. B.; Minami, H.; Okubo, M. *Macromol. Theory Simul.* **2006**, *15*, 608.
(16) Butte, A.; Storti, G.; Morbidelli, M. *DECHEMA Monogr.* **1998**, *134*, 497–507.
(17) Tobita, H. *Macromol. Theory Simul.* **2007**, *16*, 810–823.
(18) Tobita, H.; Yanase, F. *Macromol. Theory Simul.* **2007**, *16*, 476–488.
(19) Tobita, H. *Macromol. Symp.* **2008**, *261*, 36–45.
(20) Moad, G.; Rizzardo, E.; Thang, S. H. *Aust. J. Chem.* **2006**, *59*, 669–692.
(21) Luo, Y.; Wang, R.; Yang, L.; Li, B.; Zhu, S. *Macromolecules* **2006**, *39*, 1328–1337.
(22) Prescott, S. W.; Ballard, M. J.; Rizzardo, E.; Gilbert, R. G. *Macromol. Theory Simul.* **2006**, *15*, 70–86.
(23) Simms, R. W.; Cunningham, M. F. *Macromolecules* **2007**, *40*, 860–866.
(24) Simms, R. W.; Cunningham, M. F. *Macromolecules* **2008**, *41*, 5148–5155.
(25) Wakamatsu, J.; Kawasaki, M.; Zetterlund, P. B.; Okubo, M. *Macromol. Rapid Commun.* **2007**, *28*, 2346–2353.
(26) Delaittre, G.; Charleux, B. *Macromolecules* **2008**, *41*, 2361–2367.
(27) Maehata, H.; Buragina, C.; Cunningham, M.; Keoshkerian, B. *Macromolecules* **2007**, *40*, 7126–7131.
(28) Goto, A.; Fukuda, T. *Prog. Polym. Sci.* **2004**, *29*, 329–385.
(29) Hui, A. W.; Hamielec, A. E. *J. Appl. Polym. Sci.* **1972**, *16*, 749–769.
(30) Khuong, K. S.; Jones, W. H.; Pryor, W. A. *J. Am. Chem. Soc.* **2005**, *127*, 1265–1277.
(31) Matyjaszewski, K.; Qui, J.; Tsarevsky, N. V.; Charleux, B. *J. Polym Sci., Part A: Polym. Chem.* **2000**, *38*, 4724.
(32) Qui, J.; Pintauer, T.; Gaynor, S. G.; Matyjaszewski, K.; Charleux, B.; Vairon, J.-P. *Macromolecules* **2000**, *33*, 7310.
(33) Kagawa, Y.; Zetterlund, P. B.; Minami, H.; Okubo, M. *Macromolecules* **2007**, *40*, 3062–3069.
(34) Heath, M. T. *Scientific Computing: An Introductory Survey*, 2nd ed.; McGraw-Hill: Boston, 2002.
(35) Zetterlund, P. B.; Yamazoe, H.; Yamada, B.; Hill, D. J. T.; Pomery, P. J. *Macromolecules* **2001**, *34*, 7686–7691.
(36) Buback, M.; Egorov, M.; Gilbert, R. G.; Kaminsky, V.; Olaj, O. F.; Russell, G. T.; Vana, P.; Zifferer, G. *Macromol. Chem. Phys.* **2002**, *203*, 2570–2582.
(37) Russell, G. T. *Aust. J. Chem.* **2002**, *55*, 399–414.
(38) Buback, M.; Gilbert, R. G.; Hutchinson, R. A.; Klumperman, B.; Kuchta, F. D.; Manders, B. G.; O'Driscoll, K. F.; Russell, G. T.; Schweer, J. *Macromol. Chem. Phys.* **1995**, *196*, 3267–3280.
(39) Buback, M.; Kowollik, C.; Kurz, C.; Wahl, A. *Macromol. Chem. Phys.* **2000**, *201*, 464–469.

MA900035X